Supplementary Material

Radiocarbon measurements

The radiocarbon data from core MD07-3076, and the chronology for these data, are described in detail by (Skinner et al., 2010). Mixed benthic- and monospecific planktonic foraminifer samples were hand picked from core MD07-3076, cleaned using a method originally developed for Mg/Ca measurements (Barker et al., 2005), graphitized by hydrogen reduction over an iron catalyst (Vogel et al., 1984) and analysed using a National Electrostatics Corporation (NEC) Single Stage Accelerator Mass Spectrometer (SS-AMS) at the Australian National University (Fallon et al., 2010).

Benthic foraminifer radiocarbon ages can be used to provide a variety of different types of 'radiocarbon ventilation age' estimates (see e.g. Skinner and Shackleton, 2004). The radiocarbon age difference between contemporary benthic and planktonic (near-surface dwelling) foraminifera (B-P) provides an estimate of the radiocarbon age gradient across the water column at the core location (Broecker, 1989), while the radiocarbon age difference between benthic foraminifera and the contemporary atmosphere (B-Atm) provides an estimate of the true mean radiocarbon age of the deep ocean at a given location. The difference between B-Atm ventilation ages and B-P ventilation ages in a given context therefore reflects the radiocarbon age of the near-surface habitat of the planktonic foraminifera, or the surface 'reservoir age'. Published B-P ventilation age estimates (i.e. where no information on past surface reservoir ages has been advanced) may be converted to B-Atm estimates by the addition of a suitable surface reservoir age estimate. Whereas in cores MD07-3076 and MD99-2334K, direct estimates of surface reservoir ages have been obtained (Skinner et al., 2010), B-Atm ventilation age estimates from other cores referred to in the text (Figures 3, 4, and DR1) have been derived using published B-P offsets and an assumed constant (modern) surface reservoir age. The reservoir ages that have been applied to B-P estimates from cores GGC6 (Roberts et al., 2010), TR163-31B (Shackleton et al., 1988) and ODP887 (Galbraith et al., 2007) are 520, 550 and 550 years respectively.

Nd isotopes in fish debris and benthic foraminifera

Foraminifer samples were cleaned via a multi-stage mechanical and chemical cleaning protocol (Vance and Burton, 1999), prior to the separation of Nd using Eichrom transuranic-specific and lanthanide-specific resins. Hydrazine was omitted from the 'reductive' step on the basis of cleaning tests indicating no discernable cleaning effect of this hazardous and carcinogenic chemical (e.g. Yu et al., 2007). No other changes were made to the cleaning protocol, in order to maintain consistency with standard procedures. Fish debris samples were cleaned of detrital contaminants and subjected to an oxidative step only, prior to dissolution and Nd separation. All Nd isotope analyses were carried out at the University of Bristol on a Finnigan Neptune multicollector ICP-MS, following the procedure detailed in (Vance and Thirwall, 2002). Reproducibility of the Nd isotopic analyses was monitored via 15-25 separate measurements of the La Jolla standard during each analytical session and was between 0.11 and 0.17 epsilon units (2σ). Errors on the samples analysed here are dominated not by this small uncertainty due to reproducibility but by the limit imposed by low signal intensities from small samples (these higher uncertainties are those plotted in the figures).

Fish teeth/debris have a long-standing pedigree as a robust recorder of seawater Neodymium (Nd) isotope values (Martin et al., 2010). Previous work has shown that Nd is rapidly taken up and concentrated in the biogenic apatite matrix of fish debris during early diagenesis, and that the very strong partitioning of Nd into phosphate limits or precludes later significant

post-depositional alteration of the initially incorporated Nd isotopic composition (Martin et al., 2010).

Benthic foraminifera are a relatively novel substrate for the reconstruction of past seawater Nd isotopes. Any Nd associated with the precipitation of benthic foraminiferal calcite should be indistinguishable from Nd that later accumulates in association with ferromanganese oxide formation and/or adsorbtion from seawater/pore-water during early diagenesis. The resulting expectation that the Nd isotopic composition of benthic foraminifera will reflect deep-water values is supported by core-top evidence (Klevenz et al., 2008). In Figure DR1 we present additional core-top data from the North Atlantic, Southern Ocean and eastern equatorial Pacific that illustrates the fidelity of benthic foraminifera as recorders of sea-water Nd isotopes.

In contrast to leaching methods that target dispersed ferromanganese oxides within the sediment (e.g. Rutberg et al., 2000; Gutjahr et al., 2007), the analysis of Nd isotopes in both fish debris and benthic foraminifera has the advantage of avoiding the possibility (however remote) of any contamination from 'labile' sedimentary phases, such as volcanic glass or 'pre-formed' detrital oxides (Bayon et al., 2004). Nevertheless, it remains possible that even these substrates could record 'non-seawater' Nd isotope values. Although this has not yet been documented, it could in theory arise if the Nd isotopic composition of the benthic boundary layer and/or of pore-waters near the sediment-water interface was altered significantly, for example by a large natural flux of Nd from labile sedimentary phases.

Arguably the hypothetical complication noted above is most likely to occur in ocean margin settings, or areas of significant river- or wind-borne sediment input. The open marine setting MD07-3076 is inherently less prone to such complications. Three additional lines of evidence support the fidelity of the benthic foraminifer and fish debris Nd isotope values from core MD07-3076: 1) the down-core fish debris and foraminifer Nd isotope values are always in close agreement, implying that benthic foraminifera do not include a 'later' diagenetic Nd component that is not also recorded by the fish debris; 2) near core-top foraminifer and fish debris Nd isotope values are in close agreement with modern seawater measurements from the Southern Ocean (Stichel et al., 2012); and 3) the carbonate content in MD07-3076 remains consistently high, suggesting limited potential for any hypothetical detrital and/or dissolution driven Nd source.

In addition, we note that the 'lock-in' timescale for the Nd isotope signal recorded by the fish debris (and therefore also the benthic foraminifera, given their close agreement) is expected to have been at least as short as the timescale of the hyrographic changes that they are presumed to record in this context. This expectation is strongly supported by the strength of partition of Nd into the biogenic apatite matrix of fish debris, as well as the observation of very rapid (centennial scale) changes in seawater Nd isotopes recorded by both fish debris and the diagenetic ferromanganese coatings on planktonic foraminifera deposited in the Northwest Atlantic across the last deglaciation (Roberts et al., 2010).

Comparison between Southern Atlantic εNd records

Figure DR2 shows a comparison between the fish debris and benthic foraminifer based data from core MD07-3076 (this study) with the reductively cleaned and 'uncleaned' planktonic foraminifer data of (Piotrowski et al., 2012) from core TNO57-21 in the Cape Basin (41.11°S, 7.91°E, 4,981 m). The evolution of Nd isotope across the early deglaciation is very similar, albeit with measured Nd isotope values at the Cape Basin site shifted by -1 epsilon

unit relative to those measured in MD07-3075 in the open sub-Antarctic Atlantic. The reason for the apparent shift in isotope values remains unexplained, and may reflect different water mass compositions at each core site (including different amounts of NDW, or Antarctic shelf water (Carter et al., 2012; Stichel et al., 2012)), subtly different non-conservative effects on local seawater Nd isotopes at each location (Arsouze et al., 2008; Rempfer et al., 2012), or indeed different non-conservative effects on shallow pore-water or benthic boundary layer Nd isotopes recorded by the foraminifera. Future work may yet resolve these large-scale and apparent time-invariant differences between the two datasets/locations. However, a key observation in the context of the current study is that both datasets suggest that absolute maximum of the NDW contribution to the deep (and abyssal) Southern Ocean across the last deglaciation did not occur during the B-A, in contrast to the radiocarbon ventilation ages recorded at each site (Barker et al., 2010; Skinner et al., 2010). Both datasets therefore agree in demonstrating that minimum radiocarbon ventilation ages at each site do not coincide with a maximum in the local contribution of NDW relative to non-NDW.

End-member changes: reservoir age versus [Nd] or εNd

Before differences in the evolution of local radiocarbon ventilation ages and local Nd isotopes can be used to infer changes in end-member reservoir age, it is first necessary to rule out the possibility of large changes in end-member Nd isotope signatures (εNd) and/or Nd concentration ([Nd]). If we consider two main deep water end-members, one representing newly exported northern deep water (NDW) and one representing 'non-NDW' (i.e. Pacific and/or southern sourced deep water), then the fraction of local water derived from NDW will be given by:

$$f_{NDW} = \frac{[Nd]_S(\varepsilon_S - \varepsilon_{site})}{[Nd]_S(\varepsilon_S - \varepsilon_{site}) - [Nd]_N(\varepsilon_N - \varepsilon_{site})} \quad (1)$$

where ε_{site} is the measured εNd at the core site, ε_N and ε_S are the NDW and non-NDW end-member εNd values respectively, and $[Nd]_N$ and $[Nd]_S$ are the average Nd concentrations of NDW and non-NDW respectively. The expected radiocarbon concentration at any location affected predominantly by these two water masses (R_{site}) will then be given by:

$$R_{site} = R_N f_{NDW} + R_S(1 - f_{NDW}) - R_\tau \quad (2)$$

where R_N and R_S are the radiocarbon concentrations corresponding to the reservoir ages of the NDW and non-NDW deep-water end-members respectively, and R_t is the total radiocarbon decay associated with the average transit time for water arriving at the site. Local radiocarbon concentrations should therefore vary as a linear function of local εNd (which is itself a function of f_{NDW}), except to the degree that the end-member Nd and/or radiocarbon signatures vary, or indeed the mean source-to-site transit time varies. Hence large discrepancies between reconstructed trends in radiocarbon and εNd should reflect changes in the end-members and/or the mean transit time. Note that radiocarbon ages vary as a logarithmic function of radiocarbon concentrations, and therefore will be expected to deviate slightly from a linear function of εNd, and will generally be biased to younger ages.

Using the above conceptual framework, it is possible to estimate the magnitude and pattern of end-member composition changes that would be required under different sets of assumptions. Note that the large number of variables in this conceptual framework requires assumptions to

be made regarding all end-member radiocarbon and Nd compositions; no single solution exists for a given observed εNd record.

For example, if it is assumed that no significant changes in end-member Nd composition occur and that the initial radiocarbon age of NDW does not change appreciably (this is, broadly speaking, the interpretation that we have adopted), the age of the non-NDW end-member can be calculated. This hypothetical scenario is shown in Figure DR2, providing one estimate of how ocean-atmosphere CO_2 exchange via the Southern Ocean and/or North Pacific (plus/minus overturning rates) may have varied across the last deglaciation, if our premises are accurate. Note that this analysis assumes that the NDW and non-NDW end-member Nd concentrations are approximately equal ($[Nd]_N/[Nd]_S \sim 1$). This conservative assumption produces more subdued variations in the inferred non-NDW end-member age that one would obtain if a higher Nd concentration was adopted for the non-NDW end-member, e.g. more in line with modern observations of the [Nd] in the deep North Pacific that would suggest $[Nd]_N/[Nd]_S$ closer to 0.3-0.5 (Grasse et al., 2012).

A contrasting scenario that might also be considered is that *only* the εNd of the NDW end-member changes (i.e. no changes in end-member radiocarbon ventilation occur). As shown in Figure DR3, such a scenario can also be reconciled with the observed radiocarbon and εNd data fromDRMD07-3076, but only if the ε Nd of the NDW end-member approaches -7 epsilon units during the B-A (i.e. reaching a value that is more positive than modern CDW). Again, our assumption of $[Nd]_N/[Nd]_S \sim 1$ renders the inferred variability of the NDW end-member more subdued that it would be if a more concentrated non-NDW end-member was assumed. It is interesting to note that the scenario shown in Figure DR3 is somewhat similar to the one tentatively proposed by (Gutjahr et al., 2008) in exhibiting a shift to less radiogenic NDW end-member εNd values after the B-A. However, the even the changes proposed by Gutjahr et al. (2008) are small enough to remain consistent with our main conclusions. ~Furthermore, a scenario as extreme as that illustrated in Figure DR3 would be in obvious conflict with data derived from manganese crusts (Foster et al., 2007), deep water corals (van de Flierdt et al., 2006) and ferromanganese coatings on planktonic foraminifera (Roberts et al., 2010), which all indicate the occurrence of deep water εNd less than -12 epsilon units in the North Atlantic, in particular during the B-A. This would strongly argue against end-member εNd changes that are as large as those illustrated in Figure DR3, and leads us to conclude that any plausible changes in end-member Nd composition would have been too small to completely account for the radiocarbon and Nd isotope data from MD07-3076, and must therefore have been accompanied by additional changes in end-member radiocarbon ages and/or mean transit times.

References

Arsouze, T., Dutay, J.-C., Kageyama, M., Lacan, F., Alkama, R., Marti, O., and Jeandel, C., 2008, A modeling sensitivity study of the influence of the Atlantic meridional overturning circulation on neodymium isotope composition at the Last Glacial Maximum: Climate of the Past, v. 4, p. 191-203.

Barker, S., Cacho, I., Benway, H.M., and Tachikawa, K., 2005, Planktonic foraminiferal Mg/Ca as a proxy for past oceanic temperatures: a methodological overview and data compilation for the Last Glacial Maximum: Quaternary Science Reviews, v. 24, p. 821-834.

Barker, S., Knorr, G., Vautravers, M., Diz, P., and Skinner, L.C., 2010, Extreme deepening of the Atlantic overturning circulation during deglaciation: Nature Geoscience, v. 3, p. 567-571.

Bayon, G., German, C.R., Burton, K.W., Nesbitt, R.W., and Rogers, N., 2004, Sedimentary Fe-Mn oxyhydroxides as paleoceanogaphic archives and the role of aeolian flux in regulating oceanic dissolved REE: Earth and Planetary Science Letters, v. 224, p. 477-492.

Broecker, W.S., 1989, Some thoughts about the radiocarbon budget for the glacial Atlantic: Paleoceanography, v. 4, p. 213-220.

Carter, P., Vance, D., Hillenbrandt, C.D., Smith, J.A., and Shoosmith, D.R., 2012, The neodymium isotopic composition of waters masses in the eastern Pacific sector of the Southern Ocean: Geochimica et Cosmochimica Acta, v. 79, p. 41-59.

Fallon, S.J., Fifield, L.K., and Chappell, J.M., 2010, The next chapter in radiocarbon dating at the Australian National University: Status report on the single stage AMS: Nuclear Instruments & Methods in Physics Research Section B-Beam Interactions with Materials and Atoms, v. 268, p. 898-901.

Foster, G.L., Vance, D., and Prytulak, J., 2007, No change in the neodymium isotope composition of deep water exported from the North Atlantic on glacial-interglacial timescales: Geology, v. 35, p. 37-40.

Galbraith, E., Jaccard, S.L., Pedersen, T.F., Sigman, D.M., Haug, G.H., Cook, M., Southon, J., and Francois, R., 2007, Carbon dioxide release from the North Pacific abyss during the last deglaciation: Nature, v. 449, p. 890-893.

Grasse, P., Stichel, T., Stumpf, R., Stramma, L., and Frank, M., 2012, The distribution of neodymium isotopes and concentrations in the Eastern Equatorial Pacific: Water mass advection versus particle exchange: Earth and Planetary Science Letters, v. 353,Äi354, p. 198-207.

Gutjahr, M., Frank, M., Stirling, C.H., Keigwin, L.D., and Halliday, A.N., 2008, Tracing the Nd isotope evolution of North Atlantic Deep and Intermediate Waters in the western North Atlantic since the Last Glacial Maximum from Blake Ridge sediments: Earth and Planetary Science Letters, v. 266, p. 61-77.

Gutjahr, M., Frank, M., Stirling, C.H., Klemm, V., van de Flierdt, T., and Halliday, A.N., 2007, Reliable extraction of a deepwater trace metal isotope signal from Fe-Mn oxyhydroxide coatings of marine sediments Chemical Geology, v. 242, p. 351-370.

Key, R.M., Kozyr, A., Sabine, C., Lee, K., Wanninkhof, R., Bullister, J.L., Feely, R.A., Millero, F.J., Mordy, C., and Peng, T.-H., 2004, A global ocean carbon climatology: Results from the Global Data Analysis Project (GLODAP): Global Biochemical Cycles, v. 18, p. 1-23.

Klevenz, V., Vance, D., Schmidt, D., and Mezger, K., 2008, Neodymium isotopes in benthic foramnifera: Core-top systematics and down-core record from the Neogene south Atlantic: Earth and Planetary Science Letters, v. 265, p. 571-587.

Martin, E.E., Blair, S.W., Kamenov, G.D., Scher, H., Bourbon, E., Basak, C., and Newkirk, D.N., 2010, Extraction of Nd isotopes from bulk deep sea sediments for paleoceanographic studies on Cenozoic time scales: Chemical Geology, v. 269, p. 414-431.

Piotrowski, A.M., Galy, A., Nicholl, J.A.L., Roberts, N., Wilson, D.J., Clegg, J.A., and Yu, J., 2012, Reconstructing deglacial North and South Atlantic deep water sourcing using foraminiferal Nd isotopes: Earth and Planetary Science Letters, v. 357, p. 289-297.

Rempfer, J., Stocker, T.F., Joos, F., and Dutay, J.C., 2012, Sensitivity of Nd isotopic composition in seawater to changes in Nd sources and paleoceanographic implications.: Journal of Geophysical Research, v. 117, p. C12020.

Roberts, N.L., Piotrowski, A.M., McManus, J.F., and Keigwin, L.D., 2010, Synchronous deglacial overturning and water mass source changes: Science, v. 327, p. 75-78.

Rutberg, R.L., Heming, S.R., and Goldstein, S.L., 2000, Reduced North Atlantic Deep Water flux to the glacial Southern Ocean inferred from neodymium isotope ratios: Nature, v. 405, p. 935-938.

Shackleton, N.J., Duplessy, J.-C., Arnold, M., Maurice, P., Hall, M.A., and Cartlidge, J., 1988, Radiocarbon age of last glacial Pacific deep water: Nature, v. 335, p. 708-711.

Siddall, M., Khatiwala, S., van de Flierdt, T., Jones, K., Goldstein, S.L., Hemming, S.R., and Anderson, R.F., 2008, Towards explaining the Nd paradox using reversible scavenging in an ocean general circulation model: Earth and Planetary Science Letters, v. 274, p. 448-461.

Skinner, L.C., Fallon, S., Waelbroeck, C., Michel, E., and Barker, S., 2010, Ventilation of the deep Southern Ocean and deglacial CO2 rise: Science, v. 328, p. 1147-1151.

Skinner, L.C., and Shackleton, N.J., 2004, Rapid transient changes in Northeast Atlantic deep-water ventilation-age across Termination I: Paleoceanography, v. 19, p. 1-11.

Stichel, T., Frank, M., Rickli, J.r., and Haley, B.A., 2012, The hafnium and neodymium isotope composition of seawater in the Atlantic sector of the Southern Ocean: Earth and Planetary Science Letters, v. 317, p. 282-294.

van de Flierdt, T., Robinson, L.F., Adkins, J.F., Hemming, S.R., and Goldstein, S.L., 2006, Temporal stability of the neodymium isotope signature of the Holocene to glacial North Atlantic: Paleoceanography, v. 21.

Vance, D., and Burton, K., 1999, Neodymium isotopes in planktonic foraminifera: a record of the response of continental weathering and ocean circulation rates to climate change: Earth and Planetary Science Letters, v. 173, p. 365-379.

Vance, D., and Thirwall, M., 2002, An assessment of mass discrimination in MC-ICPMS using Nd isotopes: Chemical Geology, v. 185, p. 227-240.

Vogel, J.S., Southon, J.R., Nelson, D.E., and Brown, T.A., 1984, Performance of catalytically condensed carbon for use in accelerator mass spectrometry: Nuclear Instruments & Methods in Physics Research Section B-Beam Interactions with Materials and Atoms, v. 5, p. 289-293.

Yu, J., Elderfield, H., Greaves, M., and Day, J., 2007, Preferential dissolution of foraminiferal calcite during laboratory reductive cleaning: Geochemistry Geophysics Geosystems, v. 8.

Table DR1. Benthic foraminifer Nd isotope data.

Core	Depth	Cal. Age	Species	eNd	2 SE
MD07 3076	3	1295.7215	Mixed benthics	-9.2	0.2
MD07-3076	25	5385.0835	Mixed benthics	-9.8	0.4
MD07 3076	41	8110.8195	Mixed benthics	-9.8	0.8
MD07 3076	57	10900.5	Mixed benthics	-8.7	0.5
MD07 3076	67	12249.99	Mixed benthics	-8.4	0.4
MD07-3076	77	13245.62	Mixed benthics	-7.5	0.2
MD07 3076	85	14128.46	Mixed benthics	-7.2	0.3
MD07 3076	85	14128.46	Gyroidinoides soldanii	-7.5	0.2
MD07 3076	89	14499.28	Gyroidinoides soldanii	-7.2	0.2
MD07 3076	89	14499.28	Mixed benthics	-7.1	0.3
MD07 3076	95	14812.57	Gyroidinoides soldanii	-6.9	0.3
MD07 3076	95	14812.57	Mixed benthics	-7.2	0.3
MD07 3076	99	15150.91	Mixed benthics	-6.7	0.3
MD07-3076	101	15518.435	Mixed benthics	-6.3	0.3
MD07-3076	103	15756.675	Mixed benthics	-6.1	0.2
MD07 3076	117	17578.115	Mixed benthics	-5.4	0.3
MD07 3076	121	18006.225	Mixed benthics	-5.7	0.3
MD07 3076	129	18718.18	Mixed benthics	-5.5	0.3
MD07 3076	137	19403.285	Mixed benthics	-5.4	0.3
MD07 3076	145	20512.28	Mixed benthics	-5.7	0.4
MD07-3076	157	22255.47	Mixed benthics	-5.5	0.2
MD07-3076	165	23550.32	Mixed benthics	-5.5	0.2

Table DR2. Fish debris Nd isotope data

Core	Depth	Cal. Age	Species	eNd	2 SE
MD07-3076	5	1469.6405	Fish debris	-9.52	0.65
MD07-3076	29	5993.319	Fish debris	-9.43	0.2
MD07-3076	39	7466.492	Fish debris	-9.64	0.2
MD07-3076	63	11651.365	Fish debris	-8.09	0.15
MD07-3076	77	13245.62	Fish debris	-7.5	0.14
MD07-3076	79	13421.085	Fish debris	-7.7	0.16
MD07-3076	83	13830.825	Fish debris	-6.86	0.19
MD07-3076	85	14128.46	Fish debris	-7.35	0.2
MD07-3076	89	14499.28	Fish debris	-7	0.2
MD07-3076	121	18006.225	Fish debris	-5.43	0.21
MD07-3076	145	20512.28	Fish debris	-5.47	0.07

Figure S1.

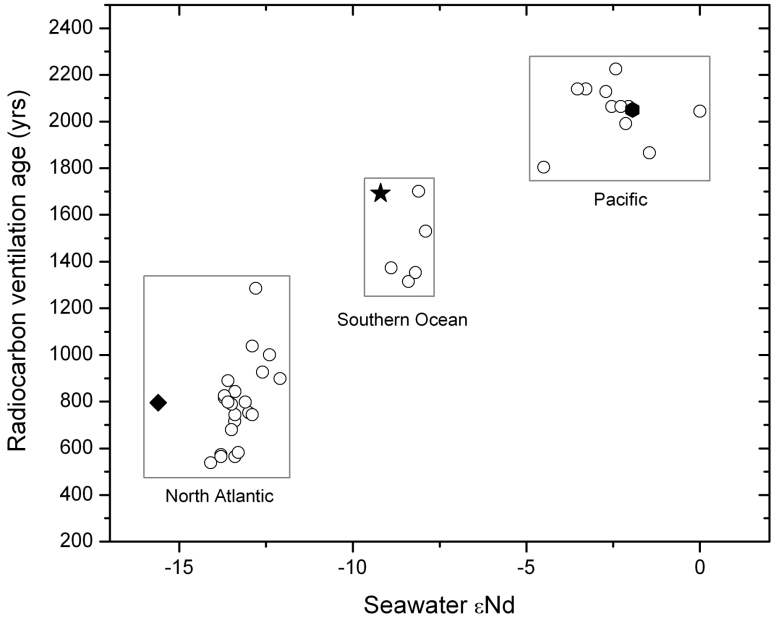

Figure DR1. Comparison of modern seawater Nd isotope data (as compiled by Siddall et al., 2008) and 'background' radiocarbon ages (relative to the pre-industrial atmosphere; i.e. equivalent to foraminiferal B-Atm estimates) (Key et al., 2004) for water samples deeper than 1500m (open circles). Boxes separate data from different ocean basins as labelled. Core-top foraminiferal Nd isotope measurements are shown for core MD07-3076 (solid star, this study; 44° 4.46'S; 14°12.47'W, 3,770m), GGC6 (solid diamond, 33°41.44'N; 57°34.56'W, 4,541m) (Roberts et al., 2010) and TR163-31B (solid hexagon, this study; 03°37'S; 83°58'W, 3,210m). Core-top radiocarbon ventilation ages (B-Atm) are based on published B-P ventilation ages plus a surface reservoir age of 520 years at the site of GGC6, 550 years at the site of TR163-31B, and 700 years at the site of MD07-3077. Analytical uncertainties (2σ) are typically less than 100 years and 1 epsilon unit.

Figure S2.

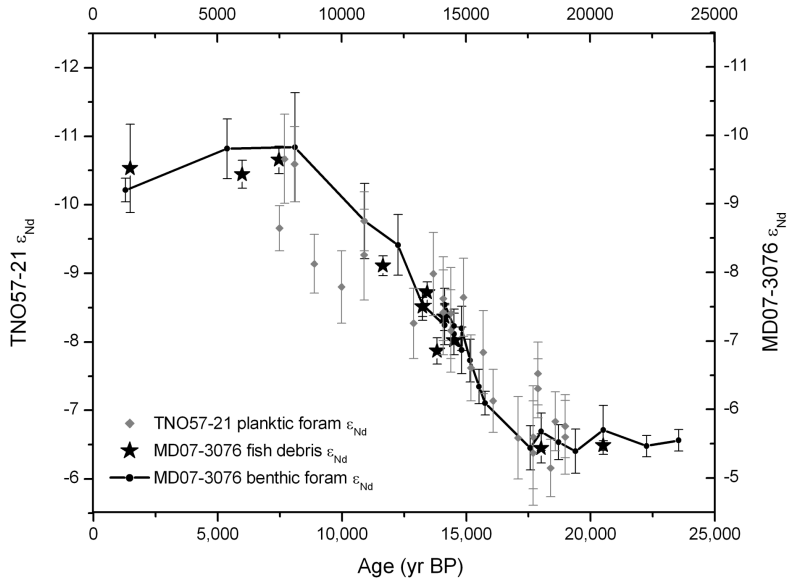

Figure DR2. Comparison of eNd records from cores MD07-3076 (this study; benthic foram data, black circles and line; fish debris data, black stars) and TNO57-21 (Piotrowski et al., 2012) (cleaned and 'uncleaned' planktonic foram data, grey circles). Note that the y-axis for the TNO57-21 data is shifted uniformly by -1 epsilon unit relative to that of the MD07-3076 data.

Figure S3.

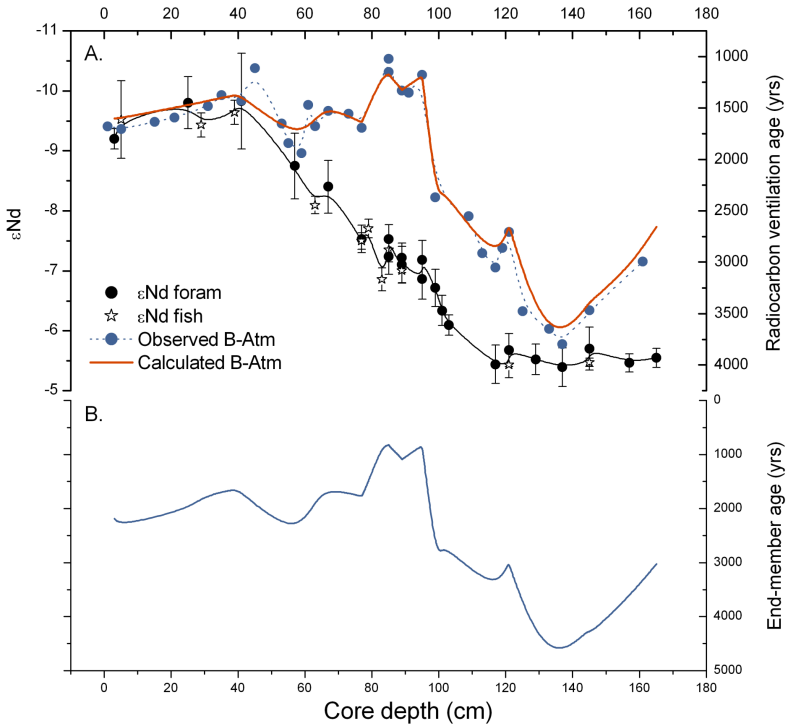

Figure DR3. Hypothetical changes in non-NDW end-member reservoir age that would reconcile the observed Nd isotope and radiocarbon ventilation records in MD07-3076, without changes in the εNd or [Nd] of either end-member. Plot A: measured Nd isotope data (open stars for fish debris; filled black circles for foraminifer analyses, black b-spline smoothed line through all data) compared with measured radiocarbon ventilation ages from MD07-3076 (filled blue circles and dashed line) and calculated radiocarbon ventilation ages (red line). The latter are based on the assumed end-member compositions shown in plot B, combined with the measured Nd isotope composition in MD07-3076. Plot B: Assumed non-NDW end-member reservoir age variability (solid blue line), based on invariant NDW end-member reservoir age (500 years) and invariant end-member Nd composition (εNd_N = -14, εNd_S = -2, $[Nd]_N/[Nd]_S \sim 1$).

Figure S4.

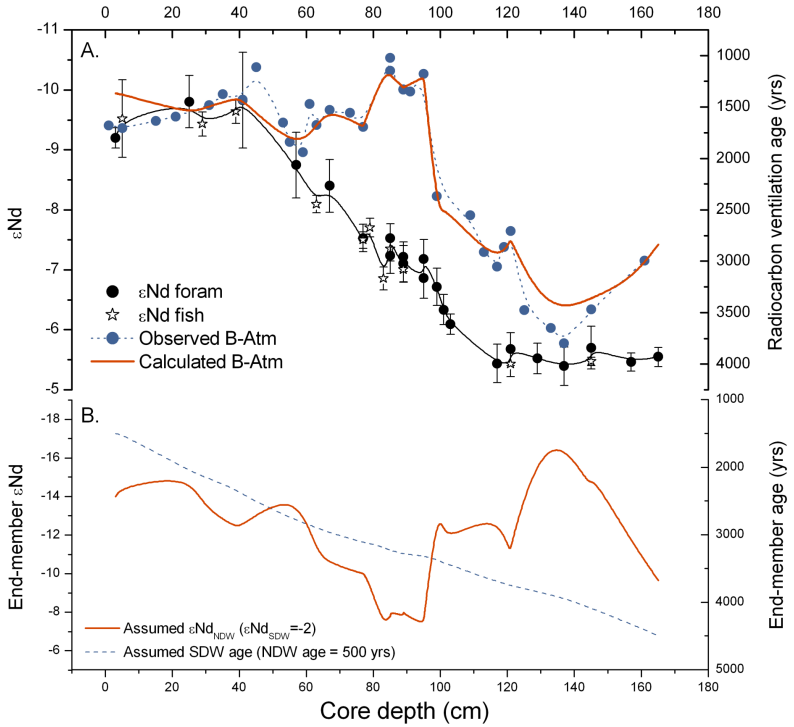

Figure DR4. Hypothetical changes in NDW end-member Nd isotope composition that would reconcile the observed Nd isotope and radiocarbon ventilation records from MD07-3076. Plot A: as for Figure S2. Plot B: Assumed NDW end-member Nd isotope composition (solid red line), and non-NDW end-member ventilation age (an arbitrary linear drift is assumed so that LGM ventilation ages greater than modern can be obtained). NDW end-member age is assumed to remain constant at 500 years, $\varepsilon Nd_S = -2$, and $[Nd]_N/[Nd]_S \sim 1$.